Available online at www.sciencedirect.com
ScienceDirect
Journal of Sound and Vibration 307 (2007) 495–512
JOURNAL OF SOUND AND VIBRATION
www.elsevier.com/locate/jsvi

Dynamic stability index and vibration analysis of a flexible Stewart platform

Parthajit Mukherjee, Bhaskar Dasgupta*, A.K. Mallik

Indian Institute of Technology Kanpur, Department of Mechanical Engineering, Kanpur 208 016, India

Received 10 January 2007; received in revised form 8 May 2007; accepted 27 May 2007

Abstract

This article proposes a dynamic stability index of a flexible manipulator. The method is illustrated by considering the 6-UPS Stewart platform as an example. First, the analysis of dynamics and vibration of a 6-UPS Stewart platform is presented. The dynamic formulation follows the Newton–Euler approach. Leg stiffness, force and torque due to viscous friction at the joints, inertia and gravity effects are considered in the model. Finally, the response of the platform, subjected to base excitations at different frequencies, has been studied and the dynamic stability index developed has been validated.

1. Introduction

Stability of a manipulator is very important for its satisfactory performance. Basic study of singularities in parallel manipulators was done by Gosselin and Angeles [1]. They classified the singularities in three types. Later, Ma and Angeles [2] showed that a highly symmetric Stewart platform (e.g., Stewart platform with regular hexagonal base and top platforms) is always singular. They called such situations as *architecture singularities*. Gosselin [3] also studied singularity associated with high condition number of force transformation matrix, which has an impact on flexible-leg Stewart platform in terms of stiffness mapping. Bhattacharya et al. [4] and Dasgupta and Mruthyunjaya [5] proposed strategies for singularity-free path planning. They used a high condition number of force transformation matrix as the representation of proximity to singularity. In all these cases, singularity studies have taken into account the architecture and configuration (i.e., kinematic parameters). The dynamic parameters (i.e., mass, inertia, stiffness, etc.) were not taken into account.

Yoshikawa [6] proposed *dynamic manipulability ellipsoid* to take care of the dynamic parameters of manipulators. It signifies, at a particular configuration, how arbitrary change in acceleration of the end-effector can be obtained with joint driving forces. Though it takes care of the inertia parameters of the manipulator, it does not consider the stiffness. Ma and Angeles [7] introduced the concept of *dynamic conditioning index* or DCI [8]. A low value of DCI signifies that the inertia matrix is close to ideal isotropic

*Corresponding author.
E-mail addresses: parthajit.mukherjee@yahoo.co.in (P. Mukherjee), dasgupta@iitk.ac.in (B. Dasgupta), akmallik@iitk.ac.in (A.K. Mallik).

0022-460X/$ - see front matter © 2007 Published by Elsevier Ltd.
doi:10.1016/j.jsv.2007.05.036

Nomenclature

$\mathbf{a}_d$, $\mathbf{a}_u$	accelerations of centres of gravity of lower and upper parts of a leg
$\mathbf{b}_i$	ith base point in the base frame
$\mathbf{B}$	base frame (attached to the reference point of the base platform)
C_u, C_p, C_s	coefficients of friction in the universal, prismatic and spherical joints, respectively
$\mathbf{D}$, $\mathbf{U}$	frames, attached to lower and upper part of the legs, respectively
F_i	magnitude of input force at ith leg
$\mathbf{F}$	force generated by actuators at the prismatic joint of legs or due to stiffness of legs
$\mathbf{F}_{\text{ext}}$	resultant of external forces acting on the moving platform
$\mathbf{g}$	acceleration due to gravity
$\mathbf{G}$	global inertial reference frame
$\mathbf{H}$	input–output force transformation matrix
$\mathbf{I}_p$	moment of inertia of the top platform including payload in platform frame
$(\mathbf{I}_{d_0})_i$, $(\mathbf{I}_{u_0})_i$	moments of inertia of lower and upper part of ith leg in local frames
$\mathbf{J}$	combined inertia of leg and moving platform
$\overline{\mathbf{k}}_i$	stationary axis of the universal joint at ith leg
$(m_d)_i$, $(m_u)_i$	masses of the lower and upper part of ith leg
M	mass of the top platform including payload
$\mathbf{M}_{\text{ext}}$	resultant of external moments acting on the moving platform
$\mathbf{p}_i$	ith platform point in the platform frame
$\mathbf{P}$	platform frame (attached to the reference point of the top platform)
$\mathbf{q}_{\mathbf{b}_i}$	$\Re_b\mathbf{b}_i$
$\mathbf{q}_{\mathbf{p}_i}$	$\Re_p\mathbf{p}_i$
$(\mathbf{r}_{d_0})_i$, $(\mathbf{r}_{u_0})_i$	centre of gravity of the lower and upper part of ith leg in local frames
$\mathbf{R}_{0p}$	centre of gravity of the top platform in platform frame
$\Re$	rotation matrix specifying the orientation of the moving platform
$\Re_b$	rotation matrix (orientation of the frame **B** with respect to frame **G**)
$\Re_p$	rotation matrix (orientation of the frame **P** with respect to frame **G**)
$\mathbf{S}_i$	vector along ith leg
$\mathbf{t}_b$	position of the frame **B** with respect to frame **G**
$\mathbf{t}_p$	position of the frame **P** with respect to frame **G**
$\dot{\mathbf{t}}_b$	linear velocity of the base platform with respect to frame **G**
$\dot{\mathbf{t}}_p$	linear velocity of the top platform with respect to frame **G**
$\ddot{\mathbf{t}}_b$	linear acceleration of the base platform with respect to frame **G**
$\ddot{\mathbf{t}}_p$	linear acceleration of the top platform with respect to frame **G**
$\mathbf{T}_i$	rotation matrix (orientation) of ith leg with respect to frame **G**
$\mathbf{u}$	centripetal acceleration of connection point of the moving platform and leg
α_b	angular acceleration of the base platform with respect to frame **G**
α_p	angular acceleration of the top platform with respect to frame **G**
η	force due to gravity, Coriolis acceleration and viscous friction at joints
ω_b	angular velocity of the base platform with respect to frame **G**
ω_p	angular velocity of the top platform with respect to frame **G**

generalized inertia matrix. For an ideal isotropic generalized inertia matrix, inertia torques are completely decoupled, wherein they are easy to control.

In the first part of this article, a dynamic stability index has been proposed that exhibits a striking analogy with the static indices and accounts for the effects of both kinematic and dynamic parameters of a manipulator. The concept and procedure are illustrated with the help of 6-UPS Stewart platform.

In literature, closed form dynamic equations of Stewart platform assuming rigid legs and stationary base were derived following three approaches, viz. Newton–Euler method [9,10], Lagrange method [11,12] and virtual work principle [13]. Shuguang and Schimmels [14] studied the behaviour of simple springs connected in parallel to a rigid body. Selig and Ding [15] developed a mathematical model of Stewart platform for the study of vibration, with simplified assumptions, namely massless legs, frictionless passive joints, etc. Lee and Geng

[16] derived the dynamic model of Stewart platform by considering flexibility of its legs and assumed the base to be static.

In the second part of the present work, generalized closed form dynamic equations of Stewart platform, following Newton–Euler approach, have been developed, considering the base movement and also accounting for the stiffness of the legs.

2. Linearization of dynamic model of Stewart platform for free vibration

The schematic diagram of a 6-UPS Stewart platform is shown in Fig. 1.

We have assumed that

(1) the base and top platforms are rigid, and
(2) legs have lumped constant stiffness (due to hydraulic actuators, material compliance, etc.) in axial direction. But they have no rotational stiffness.

The closed form dynamic equation of a 6-UPS Stewart platform with fixed base in joint space [9] is

$$\mathbf{H}^{-1}\mathbf{J}\mathbf{H}^{-\mathrm{T}}\ddot{\mathbf{L}} + \mathbf{H}^{-1}(\eta - \mathbf{J}\mathbf{H}^{-\mathrm{T}}\mathbf{u}) = \mathbf{F} + \mathbf{H}^{-1}\begin{bmatrix} \Re\mathbf{F}_{\mathrm{ext}} \\ \Re\mathbf{M}_{\mathrm{ext}} \end{bmatrix}. \tag{1}$$

In the present work, we are interested only in the platform response to initial disturbances, so we can take external loads to be zero, without losing any generality of the procedure. Therefore, we use $\mathbf{F}_{\mathrm{ext}} = \mathbf{M}_{\mathrm{ext}} = \mathbf{0}$. For free vibration, magnitude of the force in ith leg is

$$F_i = (K_{\mathrm{leg}})_i(L_i - L_{0i}) = (K_{\mathrm{leg}})_i \delta L_i, \tag{2}$$

where L_{0i} is the equilibrium length of ith leg and L_i the current length of ith leg.

For a study of the free vibration of the manipulator, η and $\mathbf{u}$ are ignored in comparison with other terms of Eq. (1). So combining Eqs. (1) and (2) we get

$$\mathbf{H}^{-1}\mathbf{J}\mathbf{H}^{-\mathrm{T}}\ddot{\mathbf{L}} = -\mathbf{K}\delta\mathbf{L}, \tag{3}$$

where $\mathbf{K} =$ diag $((K_{\mathrm{leg}})_i)$.

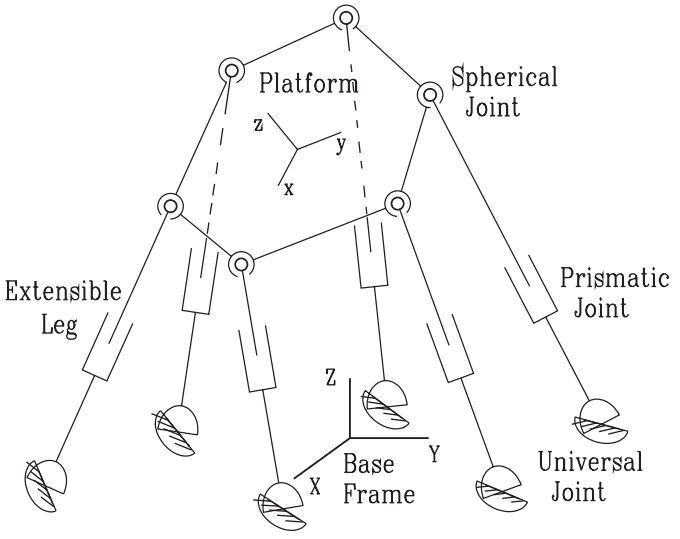

Fig. 1. The 6-UPS Stewart platform.

Here **J** and **H** both depend on the constant properties of the platforms and legs (e.g., position of platform and base joints, mass and centre of mass of moving platform and legs, etc.) as well as position and orientation (**t** and **Θ**) of the moving platform. So, natural frequencies and mode shapes of the Stewart platform also depend on position and orientation. For a particular position and orientation of a given Stewart platform, both **J** and **H** are constant. Hence $\mathbf{H}^{-1}\mathbf{J}\mathbf{H}^{-\mathrm{T}}$ is constant for that position and orientation. We denote $\mathbf{H}^{-1}\mathbf{J}\mathbf{H}^{-\mathrm{T}}$ as $\mathbf{J}_0$. Then Eq. (3) becomes

$$\mathbf{J}_0\ddot{\mathbf{L}} = -\mathbf{K}\delta\mathbf{L},$$

$$\text{or } \mathbf{J}_0\delta\ddot{\mathbf{L}} = -\mathbf{K}\delta\mathbf{L} \quad \text{as } \mathbf{L}_0 \text{ is constant.} \tag{4}$$

Assuming $\mathbf{L}e^{i\omega t}$ to be a solution of the Eq. (4), we get the generalized eigenvalue problem [17] as

$$\omega^2\mathbf{J}_0\mathbf{L} = \mathbf{K}\mathbf{L}. \tag{5}$$

Solving Eq. (5), we get *six* natural frequencies and *six* mode shapes [18–20] for a particular position and orientation of the Stewart platform.

The natural frequencies, determined from linearized dynamic model of a manipulator, incorporate the contributions of all kinematic and dynamic parameters of the manipulator. When the value of the lowest natural frequency is zero, the manipulator becomes neutrally stable and, hence, it cannot restore its position and orientation if it is perturbed by any amount. A very low value also signifies dynamic instability of the manipulator. Thus, the lowest natural frequency, calculated from Eq. (5), is an index for dynamic stability. In other words, the lowest natural frequency plays the same role in dynamic stability as does the least singular value of the force transformation matrix in statics. Being based on linearized dynamics, the stability index is essentially local, just like any criterion based on the static force transformation matrix. As such, its application in stability analysis is only in the parlance of small amplitude disturbance.

3. Simulation

The generalized eigenvalue problem (Eq. (5)) has been solved in MATLAB, taking two sets of numerical values for two different designs of the Stewart platform. Between them, one is completely general [9] and the other one is *designed* for minimum condition number of **H** [21], i.e. for best static performance. The variation of the lowest natural frequency with condition number of **H** for different mass of the moving platform (M) is shown in Figs. 2–5. Suitable stiffnesses of the legs for both the cases and dynamic parameters for the second case have been assumed. The values of the parameters are given in Appendix A.

For different poses of the Stewart platform, even though the condition number of **H** may be same, the lowest natural frequency may be different. Numerous instances of it appear in the simulation results that follow:

(1) Example 1:
   (a) *Case 1*: $M = 40\,\mathrm{kg}$.
   (b) *Case 2*: $M = 4000\,\mathrm{kg}$.
(2) Example 2:
   (a) *Case 1*: $M = 4\,\mathrm{kg}$.
   (b) *Case 2*: $M = 400\,\mathrm{kg}$.

In Figs. 2–5, large numbers of poses (configurations) are represented with their condition numbers and lowest frequencies on the two axes. We can see that the lowest natural frequency of Stewart platform decreases sharply with increase of condition number of **H**. As **H** tends towards ill-conditioning, the platform cannot support load coming from certain directions. Therefore, it gains one or more degrees of freedom. Very low value of the lowest natural frequency also signifies the instability of the moving platform.

But, at the same condition number of **H**, at different poses (different position and orientation), we see a lot of variation of the lowest natural frequency. Still, the significant *pattern* emerging in the plots between the two indices, one static and the other dynamic, shows a qualitative correlation. As such, for a pose with excellent

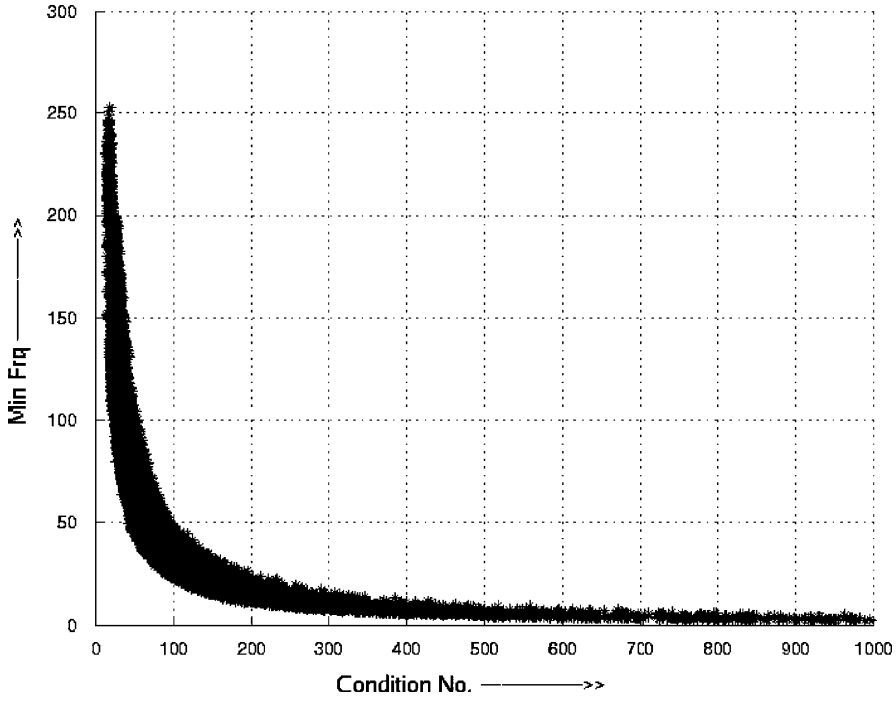

Fig. 2. Ex 1, Case 1: minimum natural frequency vs. condition number of **H**.

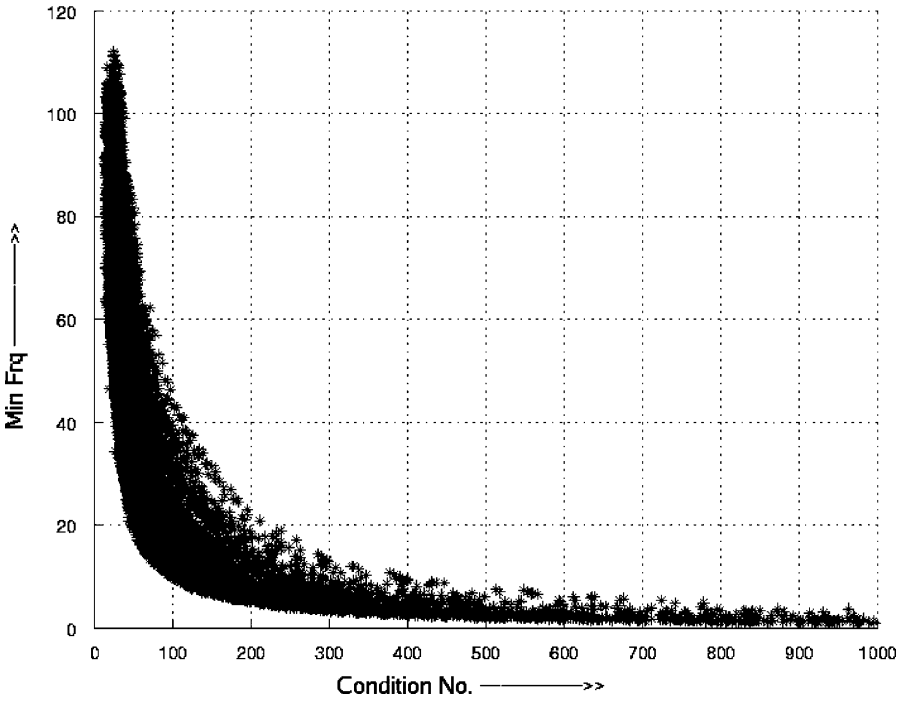

Fig. 3. Ex 1, Case 2: minimum natural frequency vs. condition number of **H**.

(low) condition number of the static transformation, typically we would expect a reasonably good (high) value of the dynamic stability index. Beyond that, the condition number of **H** alone cannot point out which position and orientation is more stable.

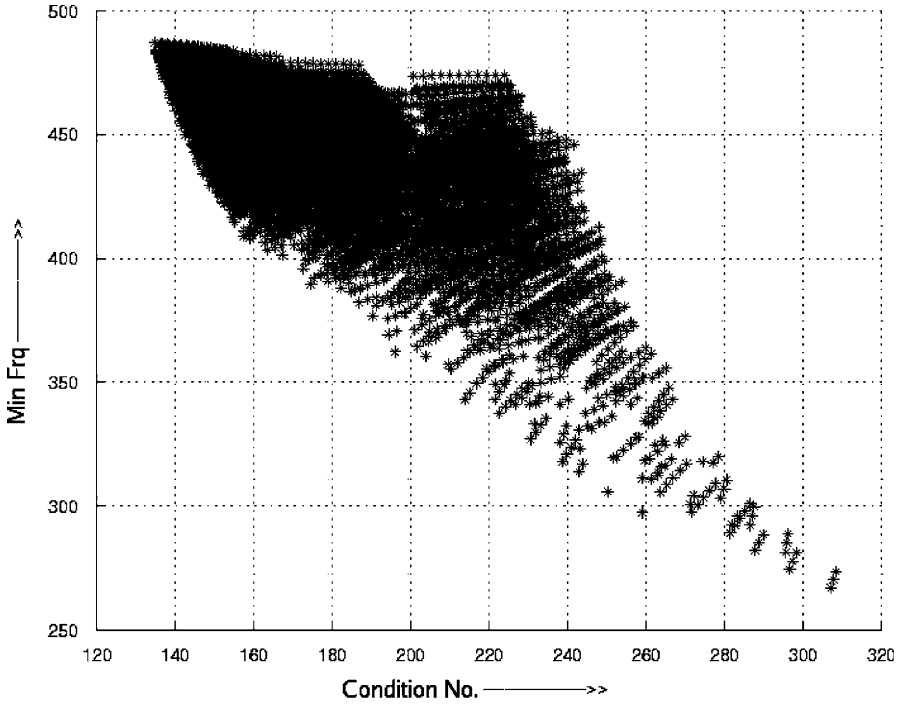

Fig. 4. Ex 2, Case 1: minimum natural frequency vs. condition number of **H**.

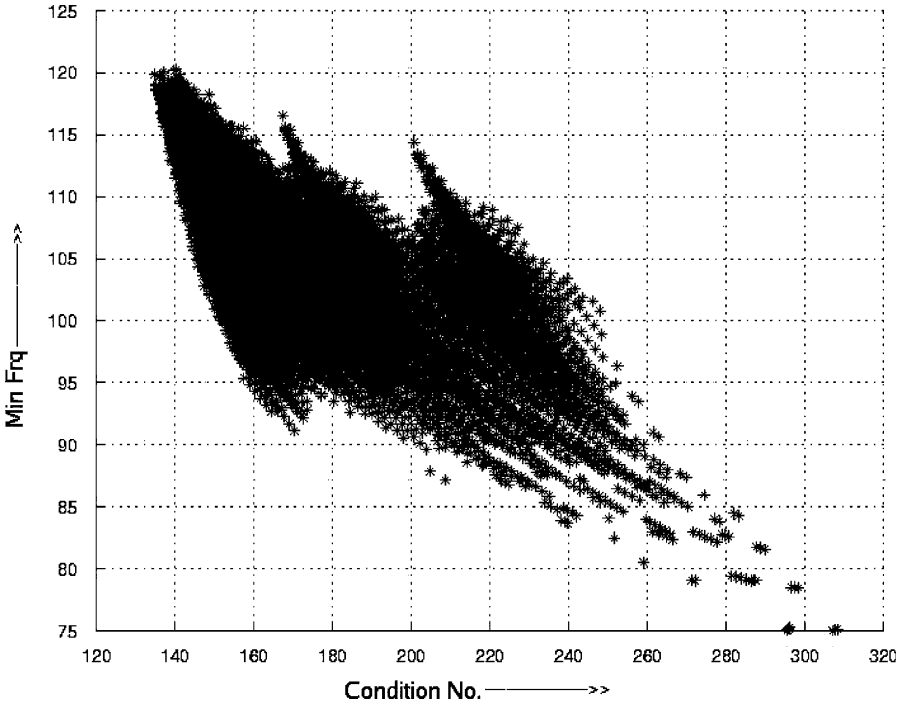

Fig. 5. Ex 2, Case 2: minimum natural frequency vs. condition number of **H**.

With the same kinematic parameters, but with different mass of the moving platform, variation of the lowest natural frequency is significant. With the change of mass of the top platform, significant change of the lowest natural frequency of the test manipulator I is clear from Figs. 2 and 3. Similarly, the variation of the

lowest natural frequency of the test manipulator II, can be seen in Figs. 4 and 5. In both the cases, the lowest natural frequency decreases with increasing mass of the platform, which signifies increasing dynamic instability of the moving platform. This effect also cannot be explained with the condition number of **H**, since **H** does not depend on dynamic parameters.

4. Closed form dynamic equation of Stewart platform with base motions and flexible legs

Dynamics of the Stewart platform is quite complicated due to its closed chain construction and six degrees of freedom. From the literature, we find that a good amount of research has been pursued to find out closed form dynamic equations of Stewart platform, following both the Newton–Euler and the Lagrangian approaches. But the effects of base motion and flexibility of the legs have not been thoroughly explored. Use of a completely general dynamic model will give better performance of the controller. Here, a generalized dynamic model of a 6-UPS Stewart platform following the Newton–Euler approach has been developed in the same way as by Dasgupta and Mruthyunjaya [9,10]. Base motion and flexibility of the legs are also considered in the present model. Leg stiffness in the axial direction is assumed to be lumped.

To develop closed form dynamic equations, first kinematics and dynamics of the legs have been studied. Then the force, applied on the top platform by each leg, and the external loads have been combined to formulate the dynamic equations of the top platform in task space. While deriving the equations of motion for a leg, the suffix i, denoting a general leg, is omitted to reduce the cluttering of the equations with too many indices. From the context, it is quite clear that this equation is for a general leg. While developing the assembled dynamic equations through the considerations of the equations of motion of the platform, the suffix i has been incorporated.

The schematic diagram of a leg and the different reference frames used for developing the dynamic equation are shown in Fig. 6.

4.1. Kinematic and dynamic analysis of a leg

Vector along a leg:

$$\mathbf{S} = (\mathbf{q_p} + \mathbf{t}_p) - (\mathbf{q_b} + \mathbf{t}_b). \tag{6}$$

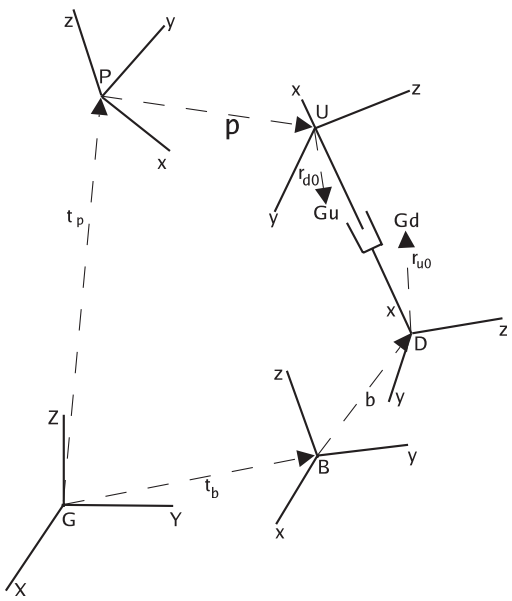

Fig. 6. Positions of reference frames.

Following the approach of Dasgupta and Mruthyunjaya [9,10] we get the relative velocity between the base point and platform point:

$$\dot{\mathbf{S}} = (\omega_p \times \mathbf{q}_p + \dot{\mathbf{t}}_p) - (\omega_b \times \mathbf{q}_b + \dot{\mathbf{t}}_b). \tag{7}$$

Similarly, the relative acceleration between the base point and platform point is found as

$$\ddot{\mathbf{S}} = [\ddot{\mathbf{t}}_p + \alpha_p \times \mathbf{q}_p + \omega_p \times (\omega_p \times \mathbf{q}_p)] - [\ddot{\mathbf{t}}_b + \alpha_b \times \mathbf{q}_b + \omega_b \times (\omega_b \times \mathbf{q}_b)]. \tag{8}$$

Let us group the velocity-dependent terms and the acceleration-dependent terms as

$$\mathbf{U}_1 = \omega_p \times (\omega_p \times \mathbf{q}_p) - \omega_b \times (\omega_b \times \mathbf{q}_b), \tag{9}$$

$$\mathbf{a}_p = \ddot{\mathbf{t}}_p + \alpha_p \times \mathbf{q}_p \quad \text{and} \tag{10}$$

$$\mathbf{a}_b = \ddot{\mathbf{t}}_b + \alpha_b \times \mathbf{q}_b. \tag{11}$$

Hence, $\ddot{\mathbf{S}}$ becomes

$$\ddot{\mathbf{S}} = \mathbf{a}_p - \mathbf{a}_b + \mathbf{U}_1. \tag{12}$$

$\ddot{\mathbf{S}}$ can be expressed in terms of leg quantities like relative sliding acceleration, angular velocity and angular acceleration as

$$\ddot{\mathbf{S}} = \ddot{L}\mathbf{s} + \mathbf{W} \times (\mathbf{W} \times \mathbf{S}) + 2\mathbf{W} \times \dot{L}\mathbf{s} + \mathbf{A} \times \mathbf{S}. \tag{13}$$

Equating $\mathbf{s} \times \ddot{\mathbf{S}}$ from both Eqs. (12) and (13) along with the relations $\mathbf{W} \cdot \mathbf{s} = 0$ and $\mathbf{A} \cdot \mathbf{s} = 0$ (Presence of a universal joint, at one end of the leg, inhibits its rotation about its own axis along the length.), we get

$$\mathbf{A} = \frac{1}{L}\mathbf{s} \times (\mathbf{a}_p - \mathbf{a}_b) + \mathbf{U}_2, \tag{14}$$

where

$$\mathbf{U}_2 = \frac{1}{L}(\mathbf{s} \times \mathbf{U}_1 - 2\dot{L}\mathbf{W}). \tag{15}$$

Accelerations of centres of gravity of lower and upper parts of the leg are

$$\mathbf{a}_d = \frac{1}{L}(\mathbf{s} \times \mathbf{a}_p) \times \mathbf{r}_d + \left[\mathbf{a}_b - \frac{1}{L}(\mathbf{s} \times \mathbf{a}_b) \times \mathbf{r}_d\right] + \mathbf{U}_3 \quad \text{and} \tag{16}$$

$$\mathbf{a}_u = (\mathbf{s} \cdot \mathbf{a}_p)\mathbf{s} + \frac{1}{L}(\mathbf{s} \times \mathbf{a}_p) \times \mathbf{r}_u + \left[\mathbf{a}_b - \frac{1}{L}(\mathbf{s} \times \mathbf{a}_b) \times \mathbf{r}_u - (\mathbf{s} \cdot \mathbf{a}_b)\mathbf{s}\right] + \mathbf{U}_4, \tag{17}$$

where

$$\mathbf{U}_3 = \mathbf{U}_2 \times \mathbf{r}_d + \mathbf{W} \times (\mathbf{W} \times \mathbf{r}_d) + \omega_b \times (\omega_b \times \mathbf{q}_b), \tag{18}$$

$$\mathbf{U}_4 = u\mathbf{s} + \mathbf{U}_2 \times \mathbf{r}_u + \mathbf{W} \times (\mathbf{W} \times \mathbf{r}_u) + 2\dot{L}\mathbf{W} \times \mathbf{s} + \omega_b \times (\omega_b \times \mathbf{q}_b). \tag{19}$$

If $\mathbf{F}_s$ is the force acting on the leg at the spherical joint, from moment equilibrium of the entire leg, we get

$$\begin{aligned}\mathbf{F}_s = {} & m_u\left[\mathbf{s} \cdot \mathbf{a}_p + \frac{1}{L}\{(\mathbf{s} \cdot \mathbf{r}_u)\mathbf{s} \cdot \mathbf{a}_p - \mathbf{r}_u \cdot \mathbf{a}_p\} - \frac{1}{L}\{(\mathbf{s} \cdot \mathbf{r}_u)\mathbf{s} \cdot \mathbf{a}_b - \mathbf{r}_u \cdot \mathbf{a}_b\}\right]\mathbf{s} \\ & - \frac{1}{L}\mathbf{s} \times \left[m_d\mathbf{r}_d \times \left\{\frac{1}{L}(\mathbf{s} \times \mathbf{a}_p) \times \mathbf{r}_d + \left(\mathbf{a}_b - \frac{1}{L}(\mathbf{s} \times \mathbf{a}_b) \times \mathbf{r}_d\right)\right\}\right. \\ & + m_u\mathbf{r}_u \times \left\{(\mathbf{s} \cdot \mathbf{a}_p)\mathbf{s} + \frac{1}{L}(\mathbf{s} \times \mathbf{a}_p) \times \mathbf{r}_u + \left(\mathbf{a}_b - \frac{1}{L}(\mathbf{s} \times \mathbf{a}_b) \times \mathbf{r}_u - (\mathbf{s} \cdot \mathbf{a}_b)\mathbf{s}\right)\right\} \\ & \left. + \frac{1}{L}(\mathbf{I}_d + \mathbf{I}_u)\mathbf{s} \times (\mathbf{a}_p - \mathbf{a}_b)\right] + \mathbf{V} - \mathbf{s}F,\end{aligned} \tag{20}$$

where

$$\mathbf{V} = (m_u \mathbf{s} \cdot \mathbf{U}_4 + C_p \dot{L} - m_u \mathbf{s} \cdot \mathbf{g})\mathbf{s} - \frac{1}{L}\mathbf{s} \times \mathbf{U}_5 \tag{21}$$

and

$$\begin{aligned}\mathbf{U}_5 = {} & m_d \mathbf{r}_d \times \mathbf{U}_3 + m_u \mathbf{r}_u \times \mathbf{U}_4 + (\mathbf{I}_d + \mathbf{I}_u)\mathbf{U}_2 \\ & + \mathbf{W} \times (\mathbf{I}_d + \mathbf{I}_u)\mathbf{W} - (m_d \mathbf{r}_d + m_u \mathbf{r}_u) \times \mathbf{g} + C_u \mathbf{W} + \mathbf{f}.\end{aligned} \tag{22}$$

Eq. (20) can be written in a compact form as

$$\mathbf{F}_s = \mathbf{Q}_p \mathbf{a}_p - \mathbf{Q}_b \mathbf{a}_b + \mathbf{V} - \mathbf{s}F, \tag{23}$$

where

$$\begin{aligned}\mathbf{Q}_p = {} & \left[m_u\left(1 + \frac{2\mathbf{s} \cdot \mathbf{r}_u}{L}\right) - \frac{m_d r_d^2 + m_u r_u^2}{L^2}\right]\mathbf{s}\mathbf{s}^{\mathrm{T}} + \frac{m_d r_d^2 + m_u r_u^2}{L}\mathbf{E}_3 - \frac{m_u}{L}(\mathbf{s}\mathbf{r}_u^{\mathrm{T}} + \mathbf{r}_u \mathbf{s}^{\mathrm{T}}) \\ & - \frac{1}{L^2}[m_d(\mathbf{s} \times \mathbf{r}_d)(\mathbf{s} \times \mathbf{r}_d)^{\mathrm{T}} + m_u(\mathbf{s} \times \mathbf{r}_u)(\mathbf{s} \times \mathbf{r}_u)^{\mathrm{T}} + \tilde{\mathbf{s}}(\mathbf{I}_d + \mathbf{I}_u)\tilde{\mathbf{s}}],\end{aligned} \tag{24}$$

$$\begin{aligned}\mathbf{Q}_b = {} & \left[m_u \frac{\mathbf{s} \cdot \mathbf{r}_u}{L} - \frac{m_d r_d^2 + m_u r_u^2}{L^2}\right]\mathbf{s}\mathbf{s}^{\mathrm{T}} + \frac{m_d r_d^2 + m_u r_u^2}{L}\mathbf{E}_3 - \frac{m_u}{L}(\mathbf{s}\mathbf{r}_u^{\mathrm{T}} + \mathbf{s}^{\mathrm{T}}\mathbf{r}_u \mathbf{E}_3) \\ & + \frac{m_d}{L}(\mathbf{r}_d \mathbf{s}^{\mathrm{T}} - \mathbf{s}^{\mathrm{T}}\mathbf{r}_d \mathbf{E}_3) - \frac{1}{L^2}[m_d(\mathbf{s} \times \mathbf{r}_d)(\mathbf{s} \times \mathbf{r}_d)^{\mathrm{T}} \\ & + m_u(\mathbf{s} \times \mathbf{r}_u)(\mathbf{s} \times \mathbf{r}_u)^{\mathrm{T}} + \tilde{\mathbf{s}}(\mathbf{I}_d + \mathbf{I}_u)\tilde{\mathbf{s}}].\end{aligned} \tag{25}$$

$\mathbf{E}_3$ is the 3×3 identity matrix and

$$\tilde{\mathbf{s}} = \begin{bmatrix} 0 & -s_z & s_y \\ s_z & 0 & -s_x \\ -s_y & s_x & 0 \end{bmatrix}.$$

Now, substituting expressions for $\mathbf{a}_p$ and $\mathbf{a}_b$ from Eqs. (10) and (11), respectively, into Eq. (23) and simplifying, we get the expression of force acting at spherical joint of the ith leg as

$$(\mathbf{F}_s)_i = (\mathbf{Q}_{\mathbf{p}i}\ddot{\mathbf{t}}_p - \mathbf{Q}_{\mathbf{b}i}\ddot{\mathbf{t}}_b) - (\mathbf{Q}_{\mathbf{p}i}\tilde{\mathbf{q}}_{pi}\alpha_p - \mathbf{Q}_{\mathbf{b}i}\tilde{\mathbf{q}}_{bi}\alpha_b) + \mathbf{V}_i - \mathbf{s}_i F_i. \tag{26}$$

4.2. Kinematics of top platform

The position vector of the centre of gravity of top platform in global reference frame is

$$\mathbf{R}_p = \mathfrak{R}_p \mathbf{R}_{0p}. \tag{27}$$

The acceleration of top platform in global reference frame is

$$\mathbf{a} = \ddot{\mathbf{t}}_p + \omega_p \times (\omega_p \times \mathbf{R}_p) + \alpha_p \times \mathbf{R}_p. \tag{28}$$

The moment of inertia of top platform including payload in global reference frame is

$$\mathbf{I} = \mathfrak{R}_p \mathbf{I}_p \mathfrak{R}_p^{\mathrm{T}}. \tag{29}$$

4.3. Dynamics of platform in task space

From force balance of the top platform, we get

$$-M\mathbf{a} + M\mathbf{g} + \mathfrak{R}_p \mathbf{F}_{\mathrm{ext}} - \sum_{i=1}^{6}(\mathbf{F}_s)_i = \mathbf{0}. \tag{30}$$

Substituting expressions of $\mathbf{a}$ and $(\mathbf{F}_s)_i$ from Eqs. (28) and (26) into Eq. (30) and simplifying,

$$\left(M\mathbf{E}_3+\sum_{i=1}^{6}\mathbf{Q}_{\mathbf{p}_i}\right)\ddot{\mathbf{t}}_p-\left(M\tilde{\mathbf{R}}_p+\sum_{i=1}^{6}\mathbf{Q}_{\mathbf{p}_i}\tilde{\mathbf{q}}_{\mathbf{p}_i}\right)\alpha_p+\sum_{i=1}^{6}\mathbf{Q}_{\mathbf{b}_i}\tilde{\mathbf{q}}_{\mathbf{b}_i}\alpha_b+M\{\omega_p\times(\omega_p\times\mathbf{R}_p)-\mathbf{g}\}-\sum_{i=1}^{6}\mathbf{Q}_{\mathbf{b}_i}\ddot{\mathbf{t}}_b+\sum_{i=1}^{6}\mathbf{V}_i=\sum_{i=1}^{6}\mathbf{s}_iF_i+\Re_p\mathbf{F}_{\text{ext}}. \tag{31}$$

Using Euler's equation for platform about the platform reference point, we have

$$-M\mathbf{R}_p\times[\ddot{\mathbf{t}}_p+\alpha_p\times\mathbf{R}_p+\omega_p\times(\omega_p\times\mathbf{R}_p)]+M\mathbf{R}_p\times\mathbf{g}-\mathbf{I}\alpha_p-\omega_p\times\mathbf{I}\omega_p+\Re_p\mathbf{M}_{\text{ext}}+\sum_{i=1}^{6}\mathbf{f}_i+\sum_{i=1}^{6}\mathbf{q}_{\mathbf{p}_i}\times(\mathbf{Q}_{\mathbf{b}_i}\ddot{\mathbf{t}}_p-\mathbf{Q}_{\mathbf{b}_i}\tilde{\mathbf{q}}_{\mathbf{b}_i}\alpha_p)-\sum_{i=1}^{6}\mathbf{q}_{\mathbf{p}_i}\times\{\mathbf{Q}_{\mathbf{p}_i}\ddot{\mathbf{t}}_p-\mathbf{Q}_{\mathbf{p}_i}\tilde{\mathbf{q}}_{\mathbf{p}_i}\alpha_p+\mathbf{V}_i-\mathbf{s}_iF_i\}=\mathbf{0}. \tag{32}$$

Again, substituting expressions of $\mathbf{a}$ and $(\mathbf{F}_s)_i$ from Eqs. (28) and (26) into Eq. (32) and simplifying, we get

$$\left(M\tilde{\mathbf{R}}_p+\sum_{i=1}^{6}\tilde{\mathbf{q}}_{\mathbf{p}_i}\mathbf{Q}_{\mathbf{p}_i}\right)\ddot{\mathbf{t}}_p-\sum_{i=1}^{6}\tilde{\mathbf{q}}_{\mathbf{p}_i}\mathbf{Q}_{\mathbf{b}_i}\ddot{\mathbf{t}}_p+\omega_p\times\mathbf{I}\omega_p+\left[\mathbf{I}+M(R_p^2\mathbf{E}_3-\mathbf{R}_p\mathbf{R}_p^{\mathrm{T}})-\sum_{i=1}^{6}\tilde{\mathbf{q}}_{\mathbf{p}_i}\mathbf{Q}_{\mathbf{p}_i}\tilde{\mathbf{q}}_{\mathbf{p}_i}\right]\alpha_p+\sum_{i=1}^{6}(\mathbf{q}_{\mathbf{p}_i}\times\mathbf{V}_i-\mathbf{f}_i)+\sum_{i=1}^{6}\tilde{\mathbf{q}}_{\mathbf{p}_i}\mathbf{Q}_{\mathbf{b}_i}\tilde{\mathbf{q}}_{\mathbf{b}_i}\alpha_p+M\mathbf{R}_p\times[(\omega_p\cdot\mathbf{R}_p)\omega_p-\mathbf{g}]=\sum_{i=1}^{6}(\mathbf{q}_{\mathbf{p}_i}\times\mathbf{s}_i)F_i+\Re_p\mathbf{M}_{\text{ext}}. \tag{33}$$

Combining Eqs. (31) and (33), we get the closed form dynamic equations of the manipulator as

$$\mathbf{J}_p\begin{bmatrix}\ddot{\mathbf{t}}_p\\ \alpha_p\end{bmatrix}-\mathbf{J}_b\begin{bmatrix}\ddot{\mathbf{t}}_b\\ \alpha_b\end{bmatrix}+\eta=\mathbf{H}\mathbf{F}+\begin{bmatrix}\Re_p\mathbf{F}_{\text{ext}}\\ \Re_p\mathbf{M}_{\text{ext}}\end{bmatrix}, \tag{34}$$

where

$$\mathbf{J}_p=\mathbf{J}_{\text{plat}}+\sum_{i=1}^{6}\mathbf{J}_{p_i},$$

$$\mathbf{J}_{\text{plat}}=\begin{bmatrix}M\mathbf{E}_3 & -M\tilde{\mathbf{R}}_p\\ M\tilde{\mathbf{R}}_p & \mathbf{I}+M(R_p^2\mathbf{E}_3-\mathbf{R}_p\mathbf{R}_p^{\mathrm{T}})\end{bmatrix},$$

$$\mathbf{J}_{p_i}=\begin{bmatrix}\mathbf{Q}_{\mathbf{p}_i} & -\mathbf{Q}_{\mathbf{p}_i}\tilde{\mathbf{q}}_{\mathbf{p}_i}\\ \mathbf{Q}_{\mathbf{p}_i}\tilde{\mathbf{q}}_{\mathbf{p}_i} & -\tilde{\mathbf{q}}_{\mathbf{p}_i}\mathbf{Q}_{\mathbf{p}_i}\tilde{\mathbf{q}}_{\mathbf{p}_i}\end{bmatrix},$$

$$\mathbf{J}_b=\sum_{i=1}^{6}\mathbf{J}_{\mathbf{b}_i},$$

$$\mathbf{J}_{b_i}=\begin{bmatrix}\mathbf{Q}_{\mathbf{b}_i} & -\mathbf{Q}_{\mathbf{b}_i}\tilde{\mathbf{q}}_{\mathbf{b}_i}\\ \tilde{\mathbf{q}}_{\mathbf{p}_i}\mathbf{Q}_{\mathbf{b}_i} & -\tilde{\mathbf{q}}_{\mathbf{p}_i}\mathbf{Q}_{\mathbf{b}_i}\tilde{\mathbf{q}}_{\mathbf{b}_i}\end{bmatrix},$$

$$\eta = \eta_{\text{plat}} + \sum_{i=1}^{6} \eta_i,$$

$$\eta_{\text{plat}} = \begin{bmatrix} M\{\omega_p \times (\omega_p \times \mathbf{R}_p) - \mathbf{g}\} \\ \omega_p \times \mathbf{I}\omega_p + M\mathbf{R}_p \times \{(\omega_p \cdot \mathbf{R}_p)\omega_p - \mathbf{g}\} \end{bmatrix},$$

$$\eta_i = \begin{bmatrix} \mathbf{V}_i \\ \mathbf{q}_{\mathbf{p}_i} \times \mathbf{V}_i - \mathbf{f}_i \end{bmatrix},$$

$$\mathbf{H} = \begin{bmatrix} \mathbf{s}_1 & \mathbf{s}_2 & \mathbf{s}_3 & \mathbf{s}_4 & \mathbf{s}_5 & \mathbf{s}_6 \\ \mathbf{q}_{\mathbf{p}_1} \times \mathbf{s}_1 & \mathbf{q}_{\mathbf{p}_2} \times \mathbf{s}_2 & \mathbf{q}_{\mathbf{p}_3} \times \mathbf{s}_3 & \mathbf{q}_{\mathbf{p}_4} \times \mathbf{s}_4 & \mathbf{q}_{\mathbf{p}_5} \times \mathbf{s}_5 & \mathbf{q}_{\mathbf{p}_6} \times \mathbf{s}_6 \end{bmatrix} \quad \text{and}$$

$$\mathbf{F} = [F_1 \quad F_2 \quad F_3 \quad F_4 \quad F_5 \quad F_6]^{\mathrm{T}}.$$

The forces, coming from the base platform and exerted by the actuators, will be transmitted to the top platform through the legs only. As the legs are flexible, there is a small relative acceleration between any two points in the legs. Hence an inertia force also appears due to it. But for a Stewart platform, constructed for practical application (for vibration isolation, tracking, sensor application, etc.), the stiffness of the legs are enough to make this inertia force negligibly small. Therefore, the net force transmitted to the top platform through a leg is equal to the force generated due to the deformation of the legs. We can get the magnitude of this force from Eq. (2).

5. Validation of the linearized model

In this section, with the help of numerical simulations of the dynamic equations developed in Section 4, we justify the linearization of the dynamic model in Section 2.

The dynamic equations of Stewart platform are found to be a *system of stiff*, *coupled*, *nonlinear*, *second order*, *ordinary differential equations* [22,23]. No analytical method is available to solve these equations. Taking *position*, *orientation*, *linear and angular velocities* as state variables, we express Eq. (34) in *state-space* as

$$\dot{\mathbf{z}} = \begin{bmatrix} \mathbf{z}(7:12) \\ \mathbf{J}_p^{-1}\left(\mathbf{HF} + \begin{bmatrix} \mathfrak{R}_p\mathbf{F}_{\text{ext}} \\ \mathfrak{R}_p\mathbf{M}_{\text{ext}} \end{bmatrix} - \eta + \mathbf{J}_b \begin{bmatrix} \ddot{\mathbf{t}}_b \\ \alpha_b \end{bmatrix}\right) \end{bmatrix}. \tag{35}$$

Here $\mathbf{z}$ is the state vector, and is given by

$$\mathbf{z} = [t_{p_x} \quad t_{p_y} \quad t_{p_z} \quad \theta_{p_x} \quad \theta_{p_y} \quad \theta_{p_z} \quad \dot{t}_{p_x} \quad \dot{t}_{p_y} \quad \dot{t}_{p_z} \quad \omega_{p_x} \quad \omega_{p_y} \quad \omega_{p_z}]^{\mathrm{T}}. \tag{36}$$

Numerical solution of Eq. (35) has been performed with the help of MATLAB tools for the test manipulator II, given in Appendix A, for the top platform's reference position, $(0, 0, 0.085)$ and orientation, $(0, 0, 0)$, subjected to base excitations in the z direction with an amplitude of 10^{-6} m and at different frequencies. We get two distinct natures of responses of the top platform, depending on whether the excitation frequencies are equal (or close) to the natural frequencies or away from them. Two typical plots, one at the second natural frequency (Fig. 7) and the other away from the natural frequencies (Fig. 8), have been shown.

For different base excitation frequencies, we get the results shown in Fig. 7 and Fig. 8, depending upon whether the frequency matches with the natural frequencies or not. For different base excitations if we plot the ratio of the response amplitude to the base excitation amplitude against the base excitation frequency, we get a plot like Fig. 9. The notion of this ratio makes sense, so long as the input (base) amplitude is small, in which case the response depends linearly on the input. From the dynamic model, it is clear that the Stewart platform has *six* natural frequencies. (With flexible legs the platform actually has infinite number of natural frequencies. However, neglecting inertia *distribution* of the legs in the approximation, it comes down to *six*.) Computations have been carried out for base excitation frequency up to a little above the second natural frequency.

The plots (Figs. 7–9) indicate that the Stewart platform resonates if the excitation is equal to the natural frequency, calculated from the linearized model. Since the foregoing simulation is based on the complete model of the manipulator, this justifies the consideration of the frequencies as representative of its dynamics.

6. Conclusions

In this paper, a generalized dynamic formulation of the 6-UPS Stewart platform has been developed using Newton–Euler approach. Effects of leg stiffness, base motion, mass and inertia of base and legs, gravitation, viscous damping all are taken into account while developing the dynamic model. This model can be used for design and control purposes. For designing a Stewart platform some forces and moments, the detailed expressions of which have not been given so far, are also necessary to be calculated to find the strength and deflection of the structure. Those can be easily found out from the forces and accelerations, already determined.

A dynamic stability index of manipulator has been developed and illustrated with the 6-UPS Stewart platform. The linearization has been validated with numerical simulations. The simulations show resonance of the complete model at the natural frequencies, which are determined through linearization. Hence these frequencies can be considered as a representative of the system dynamics. If the lowest natural frequency is very small, then the manipulator tends to be unstable and fails to support loads or to track a trajectory. Therefore, we can draw the following conclusions:

(1) Where *dynamic stability is important*, *design criterion can be maximization of the lowest natural frequency*. When we are interested in different positions and orientations, instead of a particular one, i.e. if the manipulator is going to be used in a path planning and tracking application, the design criterion can be that the lowest natural frequency is higher than a lower bound over the entire path or it should be maximized over the path in a cumulative sense with some appropriate weights. Here, more stringent first criterion needs more computational resources and also requires robust optimization procedures to solve them. To some extent, relaxation of the requirements can be made by following the second criterion. But in this case, appropriate weights should be decided based on the criticality of the operation. Over the entire path, if there are some poses where the manipulator needs to be made more stable from the application point of view, then the weight values should be high for these poses.
(2) The natural frequencies are also important for choosing the control gains. *Gains should be chosen in such a way that the closed loop poles of the corresponding linearized system do not fall near the natural frequencies*. If they fall near the natural frequencies, the controlled system may vibrate more than the uncontrolled one.
(3) From the natural frequencies, we get a rough estimate of the sampling time (Δt) for controller. For proper control, sampling time should be at most $\Delta t = 2\pi/20\omega_{n_{\max}}$ [24]. Where, $\omega_{n_{\max}}$ is the highest natural frequency.

As a natural continuation of this work, the dynamic equations developed here can be used to develop vibration controller. The gains of the controller should be such that they fall far from the natural frequencies of the linearized model. Otherwise, instead of controlling, it will induce vibration in the system. Testing of the analysis for a physical prototype may also be taken up as an experimental study, for which the formulation and results of the present simulation work is likely to provide valuable guidelines regarding choice of parameters for important and interesting revelations.

Appendix A. Description of the test manipulators

All data are in SI unit.

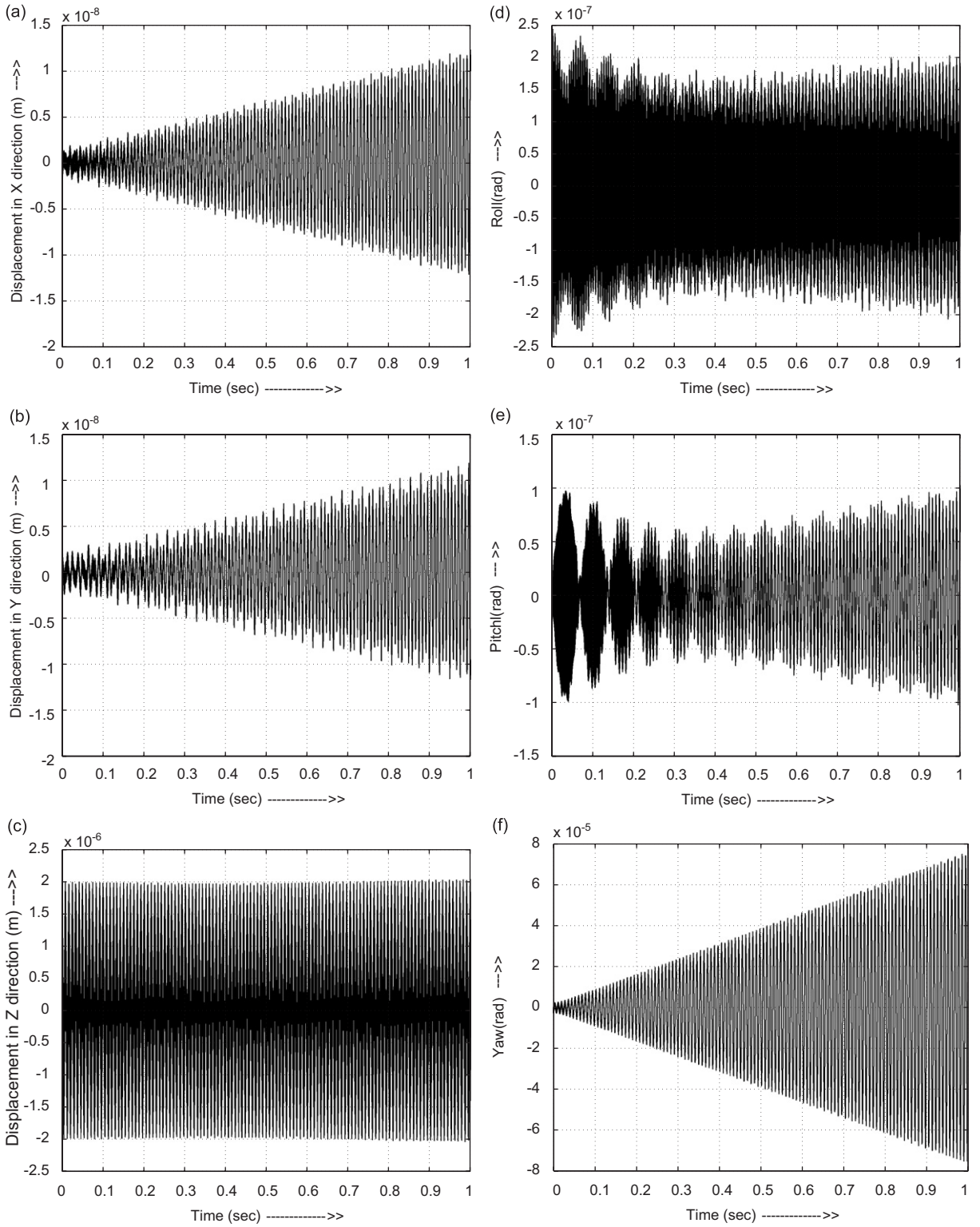

Fig. 7. Displacement from equilibrium position vs. time plot at base excitation frequency equal to 2nd natural frequency, $\omega = 749.715$ Hz: (a) translation in X direction; (b) translation in Y direction; (c) translation in Z direction; (d) rotation about X-axis; (e) rotation about Y-axis; (f) rotation about Z-axis.

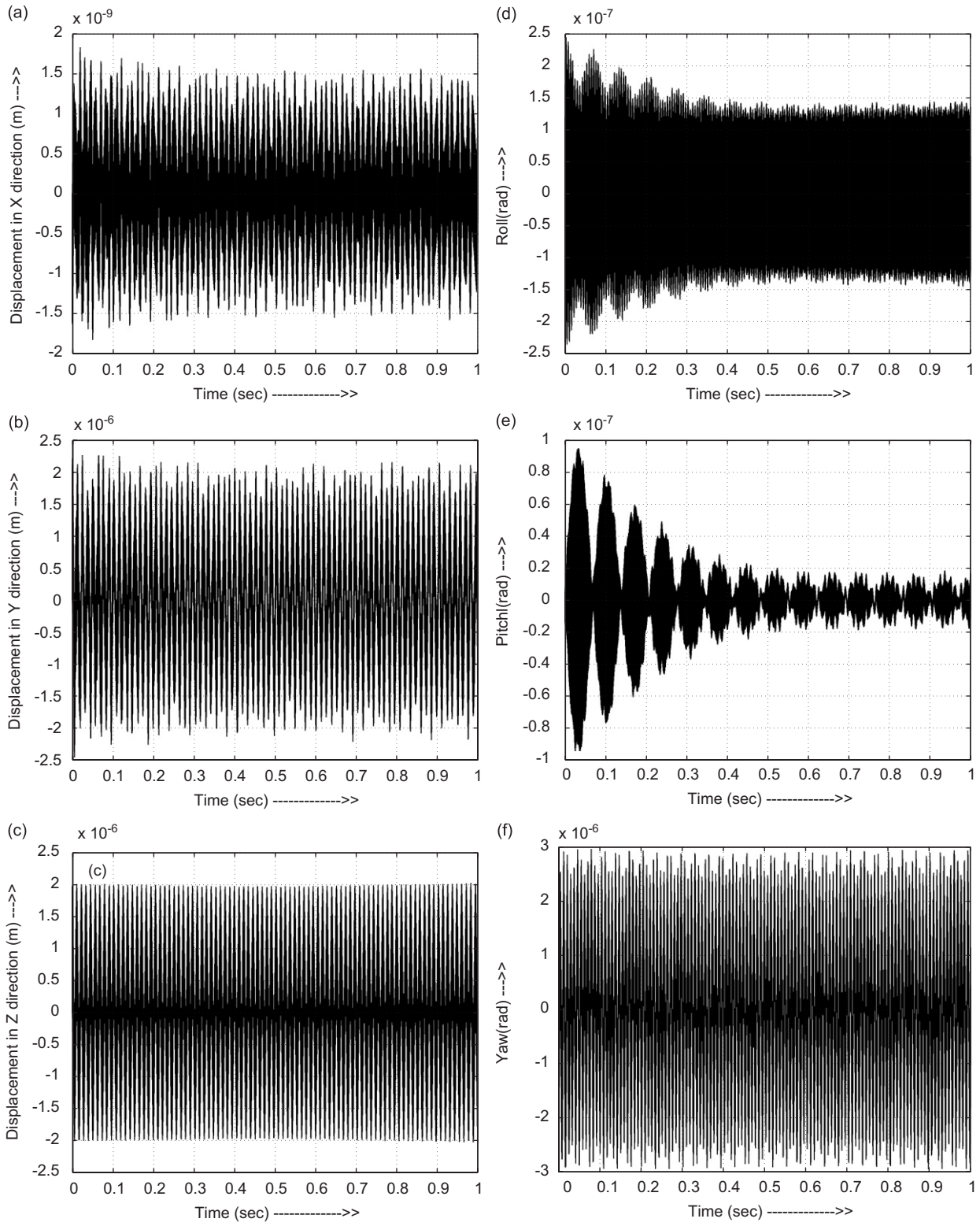

Fig. 8. Displacement from equilibrium position vs. time plot at base excitation frequency, $\omega = 550.136$, away from natural frequencies: (a) translation in X direction; (b) translation in Y direction; (c) translation in Z direction; (d) rotation about X-axis; (e) rotation about Y-axis; (f) rotation about Z-axis.

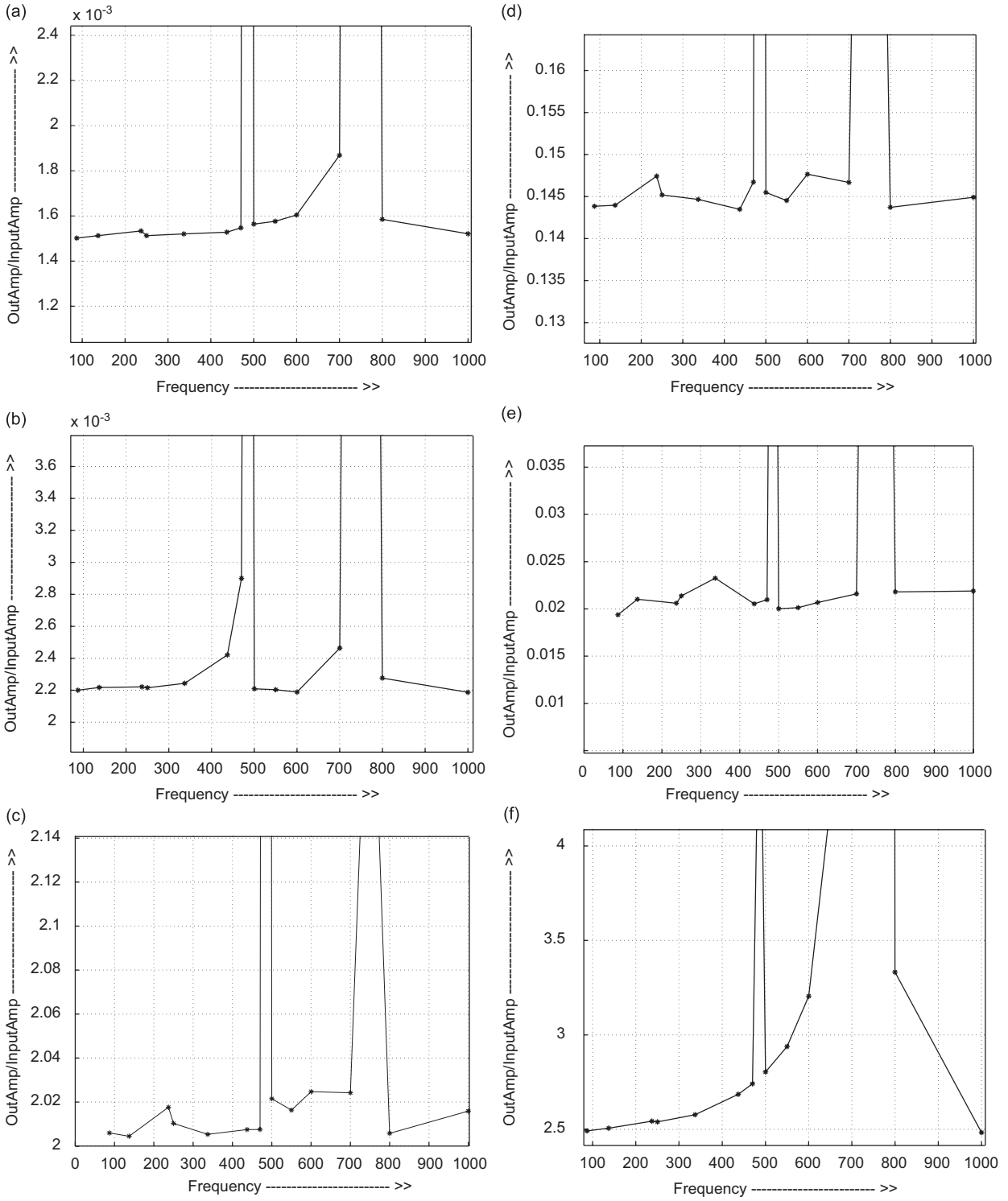

Fig. 9. Response to excitation amplitude ratio vs. excitation frequency: (a) translation in X direction; (b) translation in Y direction; (c) translation in Z direction; (d) rotation about X-axis; (e) rotation about Y-axis; (f) rotation about Z-axis.

A.1. Test manipulator I

Base points:

$$[\,\mathbf{b}_1 \quad \mathbf{b}_2 \quad \mathbf{b}_3 \quad \mathbf{b}_4 \quad \mathbf{b}_5 \quad \mathbf{b}_6\,] = \begin{bmatrix} 0.6 & 0.1 & -0.3 & -0.3 & 0.20 & 0.5 \\ 0.2 & 0.5 & 0.3 & -0.4 & -0.30 & -0.2 \\ 0.0 & 0.1 & 0.1 & 0.0 & -0.05 & 0.0 \end{bmatrix}.$$

Platform points (in platform frame):

$$[\,\mathbf{p}_1 \quad \mathbf{p}_2 \quad \mathbf{p}_3 \quad \mathbf{p}_4 \quad \mathbf{p}_5 \quad \mathbf{p}_6\,] = \begin{bmatrix} 0.3 & 0.3 & 0.0 & -0.2 & -0.15 & 0.15 \\ 0.0 & 0.2 & 0.3 & 0.1 & -0.20 & -0.15 \\ 0.1 & 0.0 & 0.0 & -0.1 & -0.05 & -0.05 \end{bmatrix}.$$

Unit vectors along fixed axes of universal joints:

$$[\,\overline{\mathbf{k}}_1 \quad \overline{\mathbf{k}}_2 \quad \overline{\mathbf{k}}_3 \quad \overline{\mathbf{k}}_4 \quad \overline{\mathbf{k}}_5 \quad \overline{\mathbf{k}}_6\,] = \begin{bmatrix} -0.8141 & 0.2308 & 0.9535 & 1.0000 & 0.7071 & -0.9535 \\ 0.2714 & 0.9231 & 0.2860 & 0.0000 & 0.7071 & 0.2860 \\ 0.0000 & 0.3077 & 0.0953 & 0.0000 & 0.0000 & -0.0953 \end{bmatrix}.$$

Mass of lower and upper part of each leg:

$$m_d = 3.0 \quad \text{and} \quad m_u = 1.0$$

Centres of gravity of lower and upper parts of each leg (in local frames):

$$\mathbf{r}_{d_0} = [\,0.4 \quad 0.14 \quad -0.18\,]^{\mathrm{T}} \quad \text{and} \quad \mathbf{r}_{u_0} = [\,-6.0 \quad -0.08 \quad 0.08\,]^{\mathrm{T}}.$$

Moments of inertia of lower and upper parts of each leg (in local frames):

$$\mathbf{I}_{d_0} = \begin{bmatrix} 0.010 & 0.005 & 0.007 \\ 0.005 & 0.002 & 0.003 \\ 0.007 & 0.003 & 0.001 \end{bmatrix} \quad \text{and} \quad \mathbf{I}_{u_0} = \begin{bmatrix} 0.005 & 0.002 & 0.002 \\ 0.002 & 0.002 & 0.001 \\ 0.002 & 0.001 & 0.003 \end{bmatrix}.$$

Centre of gravity of the platform and payload (in platform frame):

$$\mathbf{R}_0 = [\,0.04 \quad 0.03 \quad -0.06\,]^{\mathrm{T}}.$$

Moment of inertia of platform and payload (in platform frame):

$$\mathbf{I}_p = \begin{bmatrix} 0.050 & 0.003 & 0.004 \\ 0.003 & 0.040 & 0.003 \\ 0.004 & 0.003 & 0.100 \end{bmatrix}.$$

Coefficients of viscous friction:

$$C_u = 0.0001, \quad C_p = 0.001, \quad C_s = 0.0002$$

Stiffness of legs:

$$K_{\mathrm{leg}_1} = 2 \times 10^8 \quad K_{\mathrm{leg}_2} = 2 \times 10^8 \quad K_{\mathrm{leg}_3} = 2 \times 10^8,$$
$$K_{\mathrm{leg}_4} = 2 \times 10^8 \quad K_{\mathrm{leg}_5} = 2 \times 10^8 \quad K_{\mathrm{leg}_6} = 2 \times 10^8,$$

A.2. Test manipulator II

Base points:

$$[\mathbf{b}_1 \quad \mathbf{b}_2 \quad \mathbf{b}_3 \quad \mathbf{b}_4 \quad \mathbf{b}_5 \quad \mathbf{b}_6] = \begin{bmatrix} 0.03 & 0.004486 & -0.015 & -0.02793 & -0.015 & 0.02345 \\ 0.00 & 0.02966 & 0.02598 & -0.01095 & -0.02598 & -0.01872 \\ 0.00 & 0.0 & 0.0 & 0.00 & -0.0 & 0.0 \end{bmatrix}.$$

Platform points (in platform frame):

$$[\mathbf{p}_1 \quad \mathbf{p}_2 \quad \mathbf{p}_3 \quad \mathbf{p}_4 \quad \mathbf{p}_5 \quad \mathbf{p}_6] = \begin{bmatrix} 0.0428 & 0.0326 & -0.0334 & -0.0432 & -0.0094 & 0.0106 \\ 0.0139 & 0.0313 & 0.0301 & 0.0127 & -0.0440 & -0.0437 \\ 0.0 & 0.0 & 0.0 & 0.0 & 0.0 & 0.0 \end{bmatrix}.$$

Mass of lower and upper part of each leg:

$$m_d = 0.3 \quad \text{and} \quad m_u = 0.1.$$

Centres of gravity of lower and upper parts of each leg (in local frames):

$$\mathbf{r}_{d_0} = [0.04 \quad 0.014 \quad -0.018]^{\mathrm{T}} \quad \text{and} \quad \mathbf{r}_{u_0} = [-0.6 \quad -0.008 \quad 0.008]^{\mathrm{T}}.$$

Moments of inertia of lower and upper parts of each leg (in local frames):

$$\mathbf{I}_{d_0} = 10^{-5} \times \begin{bmatrix} 1.0 & 0.5 & 0.7 \\ 0.5 & 0.2 & 0.3 \\ 0.7 & 0.3 & 0.1 \end{bmatrix} \quad \text{and} \quad \mathbf{I}_{u_0} = 10^{-5} \times \begin{bmatrix} 0.5 & 0.2 & 0.2 \\ 0.2 & 0.2 & 0.1 \\ 0.2 & 100 & 300 \end{bmatrix}.$$

Centre of gravity of the platform and payload (in platform frame):

$$\mathbf{R}_0 = [0 \quad 0 \quad 0]^{\mathrm{T}}.$$

Moment of inertia of platform and payload (in platform frame):

$$\mathbf{I}_p = \begin{bmatrix} 0.0001 & 0.0 & 0.0 \\ 0.0 & 0.0001 & 0.0 \\ 0.0 & 0.0 & 0.0001 \end{bmatrix}.$$

Coefficients of viscous friction:

$$C_u = 0.0001, \quad C_p = 0.001, \quad C_s = 0.0002$$

Stiffness of legs:

$$K_{\mathrm{leg}_1} = 8 \times 10^7 \quad K_{\mathrm{leg}_2} = 8 \times 10^7 \quad K_{\mathrm{leg}_3} = 8 \times 10^7,$$
$$K_{\mathrm{leg}_4} = 8 \times 10^7 \quad K_{\mathrm{leg}_5} = 8 \times 10^7 \quad K_{\mathrm{leg}_6} = 8 \times 10^7,$$

All other parameters are the same as in the previous section.

References

[1] C. Gosselin, J. Angeles, Singularity analysis of closed-loop kinematic chains, *IEEE Transactions on Robotics and Automation* 6 (3) (1990) 281–290.
[2] O. Ma, J. Angeles, Architecture singularities of platform manipulators, *Proceedings of the IEEE International Conference on Robotics and Automation*, 1991, pp. 1542–1547.
[3] C. Gosselin, Stiffness mapping of parallel manipulators, *IEEE Transactions on Robotics and Automation* 6 (3) (1990) 377–382.
[4] S. Bhattacharya, H. Hatwal, A. Ghosh, Comparison of an exact and an approximate method of singularity avoidance in platform type parallel manipulator, *Mechanism and Machine Theory* 33 (7) (1998) 965–974.
[5] B. Dasgupta, T.S. Mruthyunjaya, Singularity-free path planning for the Stewart platform manipulator, *Mechanism and Machine Theory* 33 (6) (1998) 711–725.
[6] T. Yoshikawa, Dynamic manipulability of robot manipulators, *IEEE Conference on Decision and Control* 2 (1985) 1033–1038.

[7] O. Ma, J. Angeles, The concept of dynamic isotropy and its applications to inverse kinematics and trajectory planning, *Proceedings of the IEEE International Conference on Robotics and Automation*, Vol. 1, 1990, pp. 470–475.
[8] O. Ma, J. Angeles, Optimum design of manipulator under dynamic isotropy condition, *Proceedings of the IEEE International Conference on Robotics and Automation*, Vol. 1, 1993, pp. 470–475.
[9] B. Dasgupta, T.S. Mruthyunjaya, Closed-form dynamic equation of the general Stewart platform through the Newton–Euler approach, *Mechanism and Machine Theory* 33 (7) (1998) 993–1012.
[10] B. Dasgupta, T.S. Mruthyunjaya, A Newton–Euler formulation for the inverse dynamics of the Stewart platform manipulator, *Mechanism and Machine Theory* 33 (8) (1998) 1135–1152.
[11] G. Lebret, K. Liu, F.L. Lewis, Dynamic analysis and control of a Stewart platform manipulator, *Journal of Robotic Systems* 10 (5) (1993) 629–655.
[12] Z. Geng, L.S. Haynes, D. Lee, R.L. Carroll, On the dynamic model and kinematic analysis of a class of Stewart platforms, *Robotics and Autonomous Systems* 9 (4) (1992) 237–254.
[13] C.D. Zhang, S.M. Song, An efficient method for inverse dynamics of manipulators based on the virtual work principle, *Journal of Robotic Systems* 10 (5) (1993) 605–627.
[14] J. Shuguang, M. Schimmels, The bounds and realization of spatial stiffness achieved with simple springs connected in parallel, *IEEE Transactions on Robotics and Automation* 14 (3).
[15] J.M. Selig, X. Ding, Theory of vibration in Stewart platform, *Proceedings of the IEEE International Conference on Intelligent Robots and Systems*, Maui, Hawali, USA, 2001, pp. 2190–2195.
[16] J.D. Lee, J.Z. Geng, A dynamic model of a flexible Stewart platform, *Computers and Structures* 48 (3) (1993) 367–374.
[17] W.H. Press, S.A. Teukolsky, W.T. Vetterling, B.P. Flannery, *Numerical Recipes in C + + The Art of Scientific Computing*, second ed., Cambridge University Press, 2003.
[18] L. Meirovitch, *Analytical Methods in Vibrations*, first ed., Prentice-Hall, Englewood Cliffs, 1997.
[19] L. Meirovitch, *Elements of Vibration Analysis*, second ed., McGraw-Hill, New York, 1986.
[20] W.T. Thomson, *Theory of Vibration with Applications*, third ed., Prentice-Hall, Englewood Cliffs, 1997.
[21] T.A. Dwarkanath, B. Dasgupta, T.S. Mruthyunjaya, Design and development of a Stewart platform based force-torque sensor, *Mechatronics* 11 (7) (2001) 793–809.
[22] G.F. Simmons, *Differential Equations with Applications and Historical Notes*, second ed., McGraw-Hill, New York, 2003.
[23] E. Kreyszig, *Advanced Engineering Mathematics*, eighth ed., Wiley, New York, 2003.
[24] K.S. Fu, R.C. Gonzalez, C.S.G. Lee, *Robotics Control, Sensing, Vision and Intelligence*, first ed., McGraw-Hill Book Company, New York, 1988.